STEM CELLS AND DEVELOPMENT
Volume 30, Number 12, 2021

DOI: 10.1089/scd.2021.0058

Murine Model of Cardiac Defects Observed in Adams-Oliver Syndrome Driven by *Delta-Like Ligand-4* Haploinsufficiency

Prashan De Zoysa,[1,i] Omar Toubat,[1] Drayton Harvey,[1] Jongkyu Choi,[1,2] and S. Ram Kumar[1,3]

Heterozygous loss-of-function mutation in Delta-like ligand-4 (*Dll4*) is an important cause of Adams-Oliver syndrome (AOS). Cardiac defects, in particular outflow tract (OFT) alignment defects, are observed in about one-fourth of patients with this syndrome. The mechanism underlying this genotype-phenotype correlation has not yet been established. Dll4-mediated Notch signaling is known to play a crucial role in second heart field (SHF) progenitor cell proliferation. We hypothesized that the depletion of the SHF progenitor pool of cells due to partial loss of Dll4 is responsible for the OFT alignment defects seen in AOS. To demonstrate this, we studied Dll4 expression by murine SHF progenitor cells around E9.5, a crucial time-point in SHF biology. We used SHF-specific (Islet1-Cre) conditional knockout of *Dll4* to bypass the early embryonic lethality seen in global Dll4 heterozygotes. Dll4-mediated Notch signaling is critically required for SHF proliferation such that *Dll4* knockout results in a 33% reduction in proliferation and a fourfold increase in apoptosis in SHF cells, leading to a 56% decline in the size of the SHF progenitor pool. A reduction in SHF cells available for incorporation into the developing heart leads to underdevelopment of the SHF-derived right ventricle and OFT. Similar to the clinical syndrome, 32% of SHF-specific *Dll4* heterozygotes demonstrate foreshortened and misaligned OFT, resulting in a double outlet right ventricle. Our murine model provides a molecular mechanism to explain the cardiac defects observed in AOS and establishes a novel clinical role for Dll4-mediated Notch signaling in SHF progenitor biology.

Keywords: cardiac development, outflow tract, second heart field, SHF, Notch signaling, Delta-like ligand-4, Dll4

Introduction

During embryogenesis, the heart develops from bilateral fields of progenitor cells in the lateral plate mesoderm. The right and left first heart fields (FHF) fuse in the anterior ventral midline to form the cardiac crescent and the primitive heart tube [1]. A second set of progenitor cells from the second heart field (SHF) located dorsal to the FHF are then added to the arterial and venous poles, thereby further elongating this heart tube [2]. In the fully developed heart, whereas atria are developed with equal contributions from FHF and SHF cells, the left ventricle (LV) primarily consists of FHF cells, whereas the right ventricle (RV) and both outflow tracts (OFT) are exclusively developed from the SHF [2]. Initially, the OFT exits the primitive RV as a single vessel, and is subsequently aligned across the two ventricles, septated by neural crest cells that migrate from the neuro-ectoderm and appropriately connected to the pulmonary and systemic circulations [2].

Congenital heart defects (CHD) are the most common birth defects, occurring in roughly 1% of all live newborns [3,4]. Twenty-five percent of the newborns with CHD have a critical lesion requiring intervention before 1 year of age [3]. Given the intricate steps involved in OFT maturation, it is no surprise that OFT anomalies are encountered in 30% of all CHD [4]. One of the most common OFT abnormalities is an alignment defect in which the aorta overrides the interventricular septum [as in tetralogy of fallot (TOF)] or arises entirely from the RV [double outlet right ventricle (DORV)]. In both cases, an outlet malalignment ventricular septal defect (VSD) is also present.

It has been suggested that a genetic etiology of CHD can be determined in about 25% of patients [5]. A monogenic etiology is more frequently encountered in the setting of syndromic CHD. Adams-Oliver syndrome (AOS) is a rare congenital defect characterized by aplasia cutis congenita of the scalp and terminal transverse limb defects [6,7]. Other commonly associated anomalies include defects in the

Departments of [1]Surgery, [2]Medicine, and [3]Pediatrics, Keck School of Medicine, University of Southern California, Los Angeles, Los Angeles, California, USA.
[i]ORCID ID (https://orcid.org/0000-0002-2788-7006).

development of the central nervous system. CHD is present in about 23% of patients with AOS, with TOF being the most frequent [7]. Recently, it has been shown that mutations in Notch pathway genes are causative in AOS [7], and, in particular, heterozygous loss of Notch1 and Delta-like ligand-4 (Dll4) is sufficient to cause the disease [8–10]. Notch signaling is an evolutionarily conserved pathway that is crucial for various aspects of organ development. Dll4 was originally identified as an arterial endothelial-specific Notch ligand, and we have shown that Dll4-mediated Notch signaling plays an important role in early SHF biology [11]. We extend these findings here to show that heterozygous loss of *Dll4* in SHF cells reduces the pool of SHF progenitors available for incorporation into the developing OFT, resulting in OFT alignment defects that mirror the clinical defects encountered in AOS.

Methods

Mice

All animal experiments were carried out under protocols approved by the Institutional Animal Care and Use Committee of the University of Southern California. *Islet1-Cre* [12], and *Mef2c-AHF-Cre* [13] mouse lines have been previously described. The Cre gene was maintained on the paternal side to eliminate risk of germline transmission. $Dll4^{F/F}$ mice were generated in Duarte lab and previously reported [14–16]. *Wnt-1-Cre* [17] and tdTomato [18] mouse lines have also been previously described. Embryo dissection was carried out by standard methods. Genotyping was undertaken by using standard PCR techniques, and the specific primers used are listed in Supplementary Table S1.

Tissue analysis and histology

Immunofluorescence (IF), in situ hybridization (ISH), X-gal staining and hematoxylin-eosin stains were performed by using standard techniques. The antibodies used for staining are listed in Supplementary Table S2. Standard validation techniques included deletion of primary or secondary antibody, or use of blocking peptide to validate antibody specificity, as appropriate. The *Dll4* probe used for ISH has been previously described [14].

SHF proliferation and apoptosis were assessed by counting the number of double-positive cells in multiple high-power fields in control and mutant sections. The area in sections positive for tdTomato staining was analyzed by using ImageJ and normalized to control. In all cases, experiments were repeated in multiple sections of multiple embryos from different litters with littermate controls. For India ink injections, embryos were dissected in cold 1×PBS at embryonic day (E)10.5. Chest wall and pericardial tissues were carefully dissected to expose the heart, and glass micropipettes were used to inject ink into the primitive ventricle and OFT. Embryos were incubated in 4% paraformaldehyde overnight at 4°C. Whole-mount bright-field imaging was performed, with frontal images taken to measure the size of the RV and sagittal images taken to measure the length of the OFT in control and mutant embryos.

For all measurements, two-tailed *t*-test was used to compare significant differences at a P value <0.05.

Results

Dll4 is expressed at relevant sites and time-points in the developing heart

We evaluated Dll4 expression in the developing murine heart by using multiple modalities at embryonic stages E9.5 and E10.5, time-points of crucial relevance in SHF biology (Fig. 1). Overall, there was good correlation between Dll4 protein (IF) and transcript (ISH) expression.

Between E9–11, progenitor cells in the SHF mesoderm are rapidly proliferating and incorporating into the developing OFT. At E9.5, strong Dll4 expression was observed in

FIG. 1. Dll4 is expressed by SHF progenitor cells and SHF-derived structures in the developing heart. Representative images of E9.5 and E10.5 embryos are shown. Dll4 protein expression (IF) was studied in E9.5 transverse **(A, B)** and sagittal **(C)** fixed-frozen sections. Dll4 is expressed in the pharyngeal mesoderm in the SHF progenitor cell region **(A**, **C**, and higher magnification of *upper boxed area* of **A** in **A'**, and **C** in **C')**. Transverse sections demonstrate expression in RV endocardium and myocardium (**A**, and higher magnification of *lower boxed area* of **A** in **A"**) and developing OFT (**B**, and higher magnification of *boxed area* of **B** in **B'**). E10.5 embryos also demonstrate a similar pattern of Dll4 expression on IF **(D–F)**. Dll4 transcript expression evaluated through ISH **(G–I)** also showed an expression pattern that was similar to the Dll4 protein expression. DA (DA in **D'**, **G'**) expresses Dll4, whereas adjacent V does not. Transverse sections of SHF-lineage traced (*Islet1-Cre/R26R,tdT*) embryos were stained for Dll4 at E10.5 in more caudal splanchnic **(J)** and cranial pharyngeal **(K)** SHF mesoderm. Higher magnification of the *upper boxed area* in **J** and **K** is shown as Dll4 **(J1, K1)**, lineage-traced SHF through tdT **(J2, K2)**, and merged images **(J3, K3)** indicating co-localization of Dll4 and SHF cells. Similarly, higher magnification of the *lower boxed area* in **J** and **K** illustrates co-localization of Dll4 on SHF-derived RV **(J4–J6)** and OFT **(K4–K6)**. Transverse sections of an E10.5 embryo were co-stained for Dll4 and Islet1 **(L)**, and Dll4 and endothelial marker (CD31) **(O)**. Higher magnification of *boxed area* in **L**, and **O** is shown as Dll4 expression **(L1, O1)**, Islet1 expression **(L2)**, CD31 expression **(O2)**, and merged image **(L3, O3)**. *Inset* in L3 shows SHF cells with nuclear Islet1 expression and membranous Dll4 expression. There is co-localization of Dll4 and CD31 expression in (arterial) endothelial elements in the pharyngeal mesoderm and DA. Adjacent V is CD31-positive **(O2)**, but Dll4-negative **(O1)** confirming specificity of Dll4 signal. Transverse sections of NCC lineage-traced (*Wnt1-Cre/R26R, tdT*) embryos were stained for Dll4 at E10.5 in the cranial pharyngeal **(M)** region. Higher magnification of the *upper boxed area* in **M** is shown as Dll4 **(M1)**, lineage-traced NCC through tdT **(M2)**, and merged images **(M3)** indicating nonoverlapping expression of Dll4 and tdT. Serial transverse sections of E9.5 embryo **(N)** were stained for Dll4 and Ap2α. Higher magnification of *boxed area* in **N** is shown as Dll4 expression **(N1)**, and Ap2α expression **(N2)** in serial sections. Scale bars: 100 μm **(A'–C'**, **D'–F'**, **G'–I'**, **J1–K6**, **L1–L3**, **M4–M6**, **O1–O3)**, 250 μm **(A–O)**, and 50 μm **(M1–M3**, **N1**, **N2)**. DA, Dorsal Aorta; Dll4, delta-like ligand-4; IF, immunofluorescence; ISH, in situ hybridization; OFT, outflow tract; PM, pharyngeal mesoderm; RV, right ventricle; SHF, second heart field; V, cardinal vein.

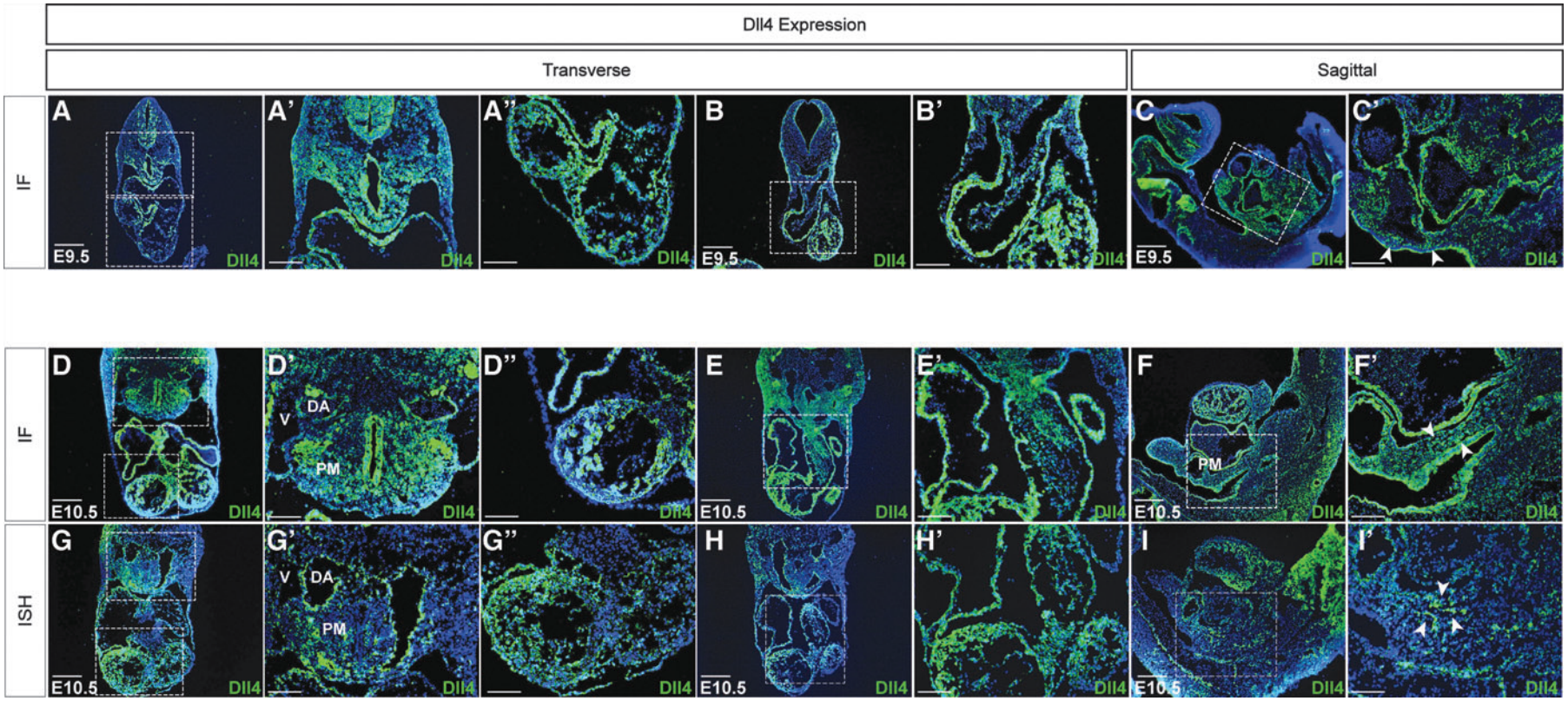
Dll4 Expression
Transverse
Sagittal
IF
ISH
A
A'
A''
B
B'
C
C'
D
D'
D''
E
E'
F
F'
G
G'
G''
H
H'
I
I'
E9.5
E10.5
Dll4
V
DA
PM

(*Continued*)

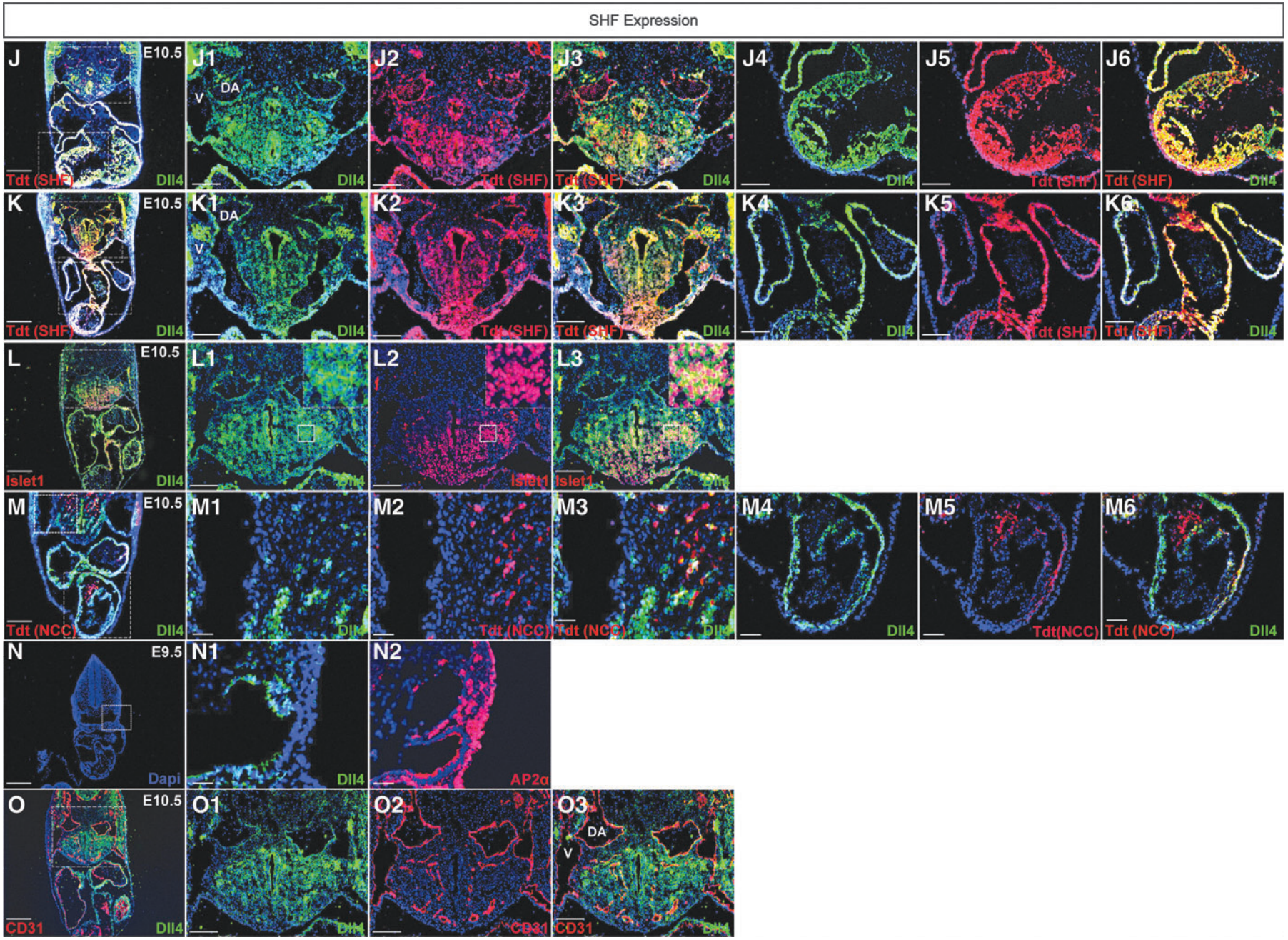

FIG. 1. (*Continued*).

the splanchnic and pharyngeal mesodermal regions. IF staining revealed broad Dll4 expression in the region of SHF progenitors in both transverse (Fig. 1A, A', B) and sagittal (Fig. 1C, C') sections. Continuing to E10.5, strong Dll4 expression could be demonstrated in the region of SHF progenitors by IF (Fig. 1D, D', E, F, F'), and ISH (Fig. 1G, G', H, I, I'). We then specifically studied expression in SHF progenitors by using two modalities to label SHF—(1) We lineage-traced SHF by breeding the Rosa26-tdTomato (*R26R,tdT*) line into *Islet1-Cre* [12] background and (2) we stained wild-type sections for Islet1, which at this stage is expressed primarily in SHF [11]. Dll4 staining in sections of E10.5 *Islet1-Cre/R26R,tdT* embryos indicated that tdT-expressing SHF cells co-expressed Dll4 in the splanchnic (Fig. 1J–J3) and pharyngeal (Fig. 1K–K3) mesodermal regions. Similarly, there was significant overlap between nuclear Islet1 expression and membranous Dll4 expression by SHF cells in the pharyngeal mesoderm (Fig. 1L–L3).

Neural crest cells travel down the pharyngeal region to reach the developing OFT. We, therefore, evaluated Dll4 expression in neural crest cells again by using both lineage-tracing (by breeding R26R,tdT line into Wnt1-Cre background) and co-staining sections with Ap2α, a marker of migratory neural crest cells. At E10.5, tdT-expressing NCC cells in the pharyngeal mesodermal region did not express Dll4 (Fig. 1M–M3). Similarly, comparable sections showed that Dll4 (Fig. 1N1) and Ap2α (Fig. 1N2) were expressed by adjacent cells in the pharyngeal region and not co-localized, indicating that the neural crest cells that are in the pharyngeal region at E9.5 do not express Dll4. Given that Dll4 is an arterial endothelial-specific protein [14], we stained E10.5 sections for the endothelial-specific marker, CD31, and Dll4. This confirmed co-expression of Dll4 and CD31 in the dorsal aorta (DA in Fig. 1O3), but a lack of Dll4 expression in the adjacent CD31-positive cardinal vein (V in Fig. 1O3), as expected. In addition, a distinct set of CD31-positive endothelial cells (likely of arterial origin) in the pharyngeal mesodermal region also expressed Dll4 (Fig. 1O–O3).

We also evaluated Dll4 expression in the developing RV and OFT, both of which are derived from SHF progenitors. At E9.5, the OFT showed prominent Dll4 expression in both endocardium and myocardium by IF (Fig. 1B, B', C, C'). This expression pattern continued to E10.5, where OFT displayed Dll4 expression by both modalities. Again, both endocardium and myocardium expressed Dll4 protein (Fig. 1E, E', F, F'). Dll4 mRNA was expressed more strongly in OFT endocardium, but some expression was also seen in the myocardium (Fig. 1H, H', I, I'). We studied Dll4 expression in the OFT of lineage-traced embryos. At E10.5, *Islet1-Cre/R26R,tdT* embryos showed that tdT-expressing SHF cells in the OFT also expressed Dll4 (Fig. 1K, K4–K6). In contrast, in *Wnt1-Cre/R26R,tdT* embryos, the Dll4-expressing cells were adjacent to, but distinct from, the tdT-expressing NCC cells in the OFT (Fig. 1M, M4–M6). At E9.5, RV endocardium and myocardium expressed Dll4 by IF (Fig. 1 A, A''). At E10.5, RV endocardium and myocardium expressed Dll4 protein (Fig. 1D, D'', J, J4), but myocardial staining was less robust. Further, *Islet1-Cre/R26R,tdT* embryos showed that tdT-expressing SHF cells in the RV also expressed Dll4 (Fig. 1J, J4–J6).

Dll4 mRNA was expressed more strongly in RV endocardium, but some expression was also seen in the myocardium (Fig. 1G, G'').

Haploinsufficiency of Dll4 in SHF disrupts OFT alignment

Global knockout of *Dll4* is embryonically lethal by E9.5 due to vascular maturation arrest [15]. Interestingly, in the same study, haploinsufficiency of Dll4 was also shown to disrupt vascular maturation with variable penetrance. In the context of SHF biology, our own previous work has shown that conditional knockout of *Dll4* expression bypasses the early lethality, allowing evaluation of cardiac development. SHF-specific *Dll4* knockout results in a spectrum of defects extending from severe lack of SHF-derived RV and OFT to a fully penetrant DORV phenotype [11]. We, therefore, wanted to study the impact of partial loss of Dll4 in SHF on OFT development.

To that end, we evaluated heterozygous *Dll4* mutation in the *Islet1* background (*Islet1-Cre,Dll4*$^{F/wt}$). Embryos were recovered in expected Mendelian numbers, indicating a lack of embryonic lethality. We studied the cardiac phenotype at E14.5 in 28 mutant embryos compared with 40 cre-negative littermate controls (Fig. 2). Nineteen out of 28 mutants had a normal cardiac phenotype. The remaining nine mutants (32%, Fig. 2D) demonstrated OFT alignment defects. There was a gradation noted in the severity of the alignment defect. Some embryos demonstrated a prominent VSD (Fig. 2B3) and the aortic valve arose entirely from the RV (Fig. 2B4 vs. A4), resembling the clinical DORV. Other mutants displayed a much shallower VSD (Fig. 2C3 compared to B3) and the aorta was over-riding the VSD (Fig. 2C4), thus having inflow from both ventricles. This lesion was reminiscent of the clinical tetralogy-style defect. In both controls and mutants, the OFT was appropriately septated. The pulmonary valve arose more cranially (indicating a normal sub-pulmonary conus) and exited the RV (Fig. 2A5, B5 and C5). There was a normal connection between the posterior outflow vessel to the systemic circulation and the cranial, anterior vessel to the pulmonary circulation, indicating appropriate rotation. Thus, our murine model phenocopies the variably penetrant alignment defect seen in patients with AOS.

A smaller subset of SHF cells expresses *Mef2c* as they exit the mesoderm to enter the developing heart. Heterozygous loss of *Dll4* in Mef2c-expressing SHF cells does not result in a cardiac phenotype (Fig. 2D), indicating that the timing and degree of Dll4 loss plays a role in the ultimate cardiac phenotype. Because *Islet1*-driven cre recombinase may also be active in a subset of NCC, we wanted to confirm that the observed defects in *Islet1-Cre* mice were not neural-crest driven. To that end, we studied the effect of Dll4 loss in *Wnt1-Cre* mice. Both heterozygous (Fig. 2E1, E2) and homozygous (Fig. 2F1, F2) loss of *Dll4* in Wnt1-expressing NCC does not result in a discernable cardiac phenotype, consistent with a lack of expression of Dll4 in NCC.

To study the developmental defect resulting in the observed cardiac phenotype, we examined heterozygous mutant embryos at E10.5 when early cardiac assembly is completed. We used the *Islet1-Cre/R26R,tdT* mice to label the RV and OFT and also injected India ink into the RV of wildtype embryos as a complementary technique to visualize the OFT

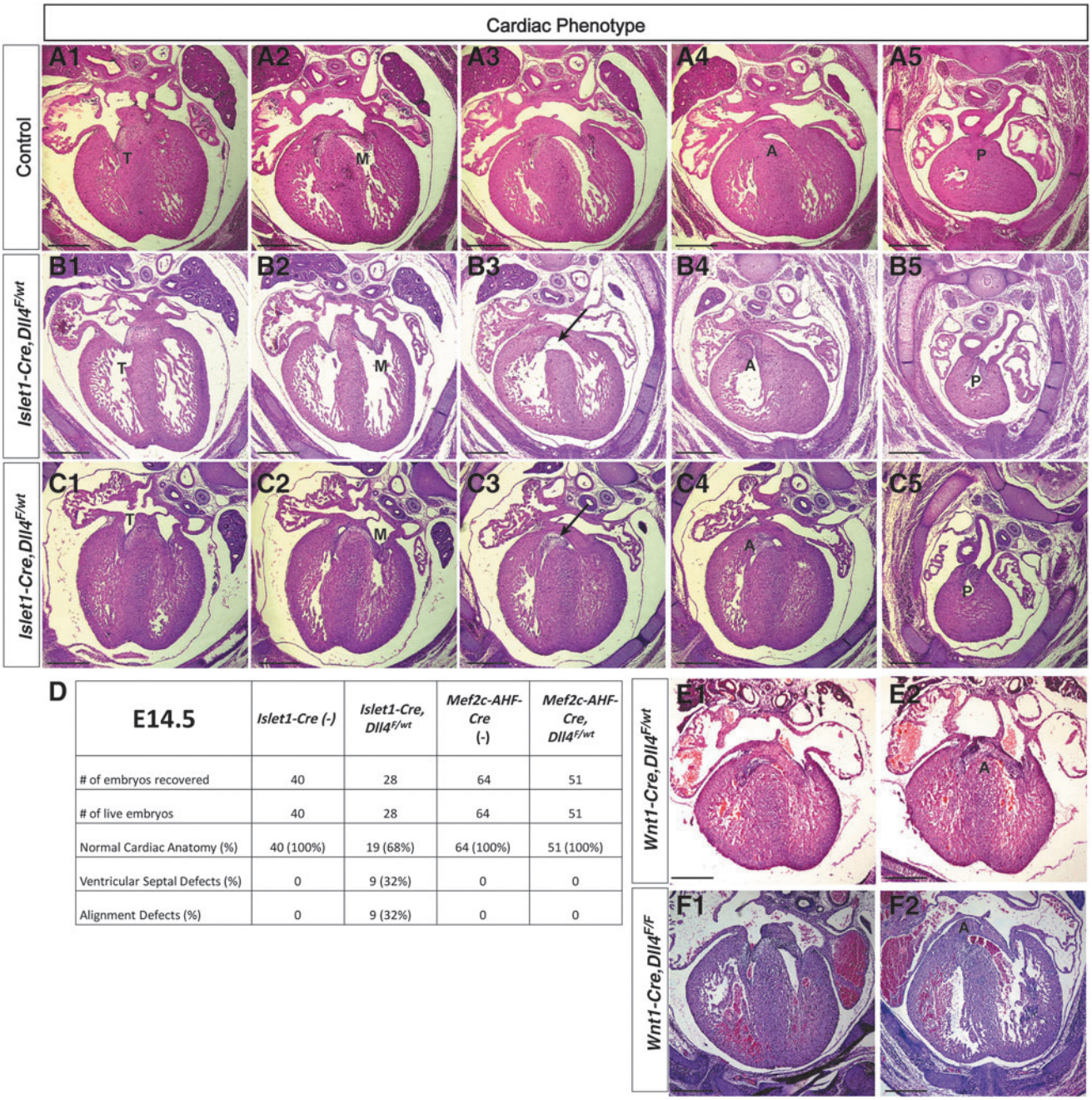

FIG. 2. Haploinsufficiency of Dll4 in SHF results in misalignment of OFT. Heterozygous conditional loss of Dll4 expression in SHF was achieved by using Islet1-mediated cre expression. Hematoxylin and eosin-stained transverse sections of E14.5 cre-negative littermate control embryos and Dll4 heterozygous mutants (*Islet1-Cre,Dll4$^{F/wt}$*) show properly developed T **(A1, B1, C1)** and M **(A2, B2, C2)** valves. A third of the mutants demonstrated an outlet VSD **(*A*rrows** in **B3, C3)** compared to intact septum in controls **(A3)**. The A arises entirely from the RV in a subset of mutant embryos **(B4)** and overrides the VSD in the other **(C4)**. In both control and mutant embryos, the P exits the RV **(A5, B5, C5)**. (**D**) Indicates the number and phenotypes of embryos recovered among the different genotypes mentioned. Dll4 heterozygous and homozygous mutants in *Wnt1* background (*Wnt1-Cre,Dll4$^{F/wt}$*, E1, E2 and *Wnt1-Cre, Dll4$^{F/F}$*, F1, F2) demonstrate normal heart phenotype at E14.5. Scale bar—300 μm **(A1–C5, E1–F2)**. A, aortic valve; M, mitral valve; P, pulmonary valve; T, tricuspid valve; VSD, ventricular septal defect.

(Fig. 3). All embryos demonstrated appropriate early assembly at this stage. We noticed a gradation in reduction in RV size and OFT length in mutant embryos. Overall, India ink filled RV was 42% smaller in mutants compared with controls (Fig. 3A, A', B), whereas the corresponding tdT-labeled RV was 48% smaller in mutants compared with controls (Fig. 3C, C', D). Similarly, the percentage of ventricular area occupied by tdT-labeled cells (indicating RV portion of the ventricles indexed for LV) was 56% reduced in mutant sections compared with control (Fig. 3E, E', F). The length of the OFT was 30% reduced in India ink labeled whole mounts of mutants compared with control embryos

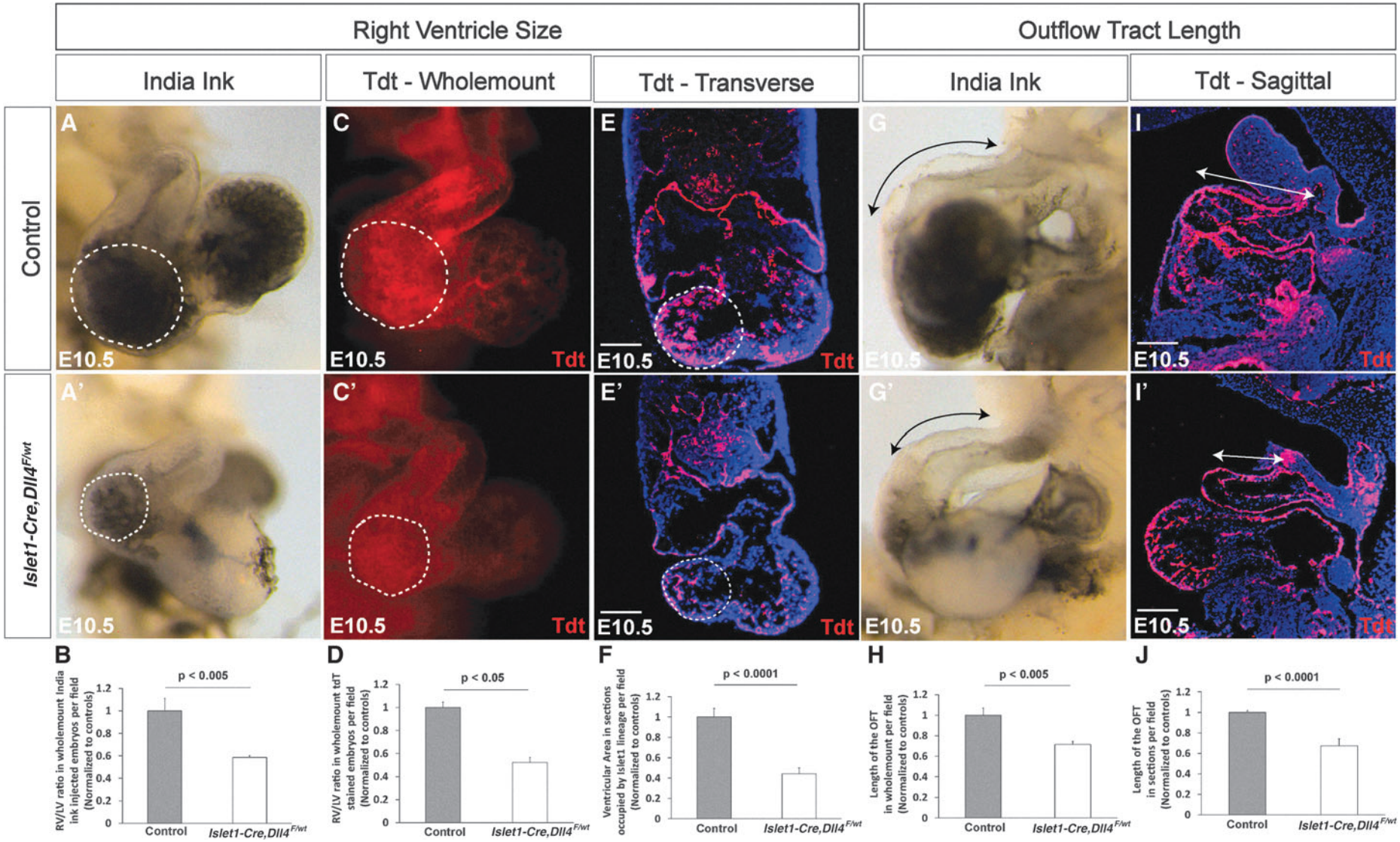

FIG. 3. Haploinsufficiency of Dll4 in SHF leads to a reduced size of RV and foreshortened OFT. Heterozygous conditional loss of *Dll4* expression in SHF progenitor cells was achieved by using Islet1-mediated cre expression. Whole-mount examination at E10.5 of India ink injected control wildtype embryos **(A)** and Islet1 lineage-traced control embryos **(C)** compared with their respective *Dll4* heterozygous mutants **(A', C')** demonstrates a hypoplastic RV in the mutants. Area (mean, SEM) of the RV in India ink injected whole-mount embryos (2 control and 5 mutant, **B**) and lineage-traced tdT-positive RV (2 control and 2 mutant, **D**) was compared with area of the corresponding LV and normalized to control embryos. This shows an almost 50% reduction in the RV/LV ratio in mutants [$P < 0.005$ **(B)** and $P < 0.05$ **(D)** by unpaired two-tailed *t*-test]. tdT-positive RV area within the entire ventricular area (10 control, **E** and 14 mutant transverse sections, **E')** was measured and normalized to control embryo sections **(F)**. This shows a 56% reduction of the RV in mutants compared with controls ($P < 0.0001$ by unpaired two-tailed *t*-test). Length (mean, SEM) of India ink injected OFT was measured in whole-mount embryos (8 control, **G** and 14 mutant, **G')** and Islet1 lineage-traced tdT-positive sagittal sections (7 control, **I** and 5 mutant, **I')** and normalized to control embryos. This shows a 30%–33% reduction in OFT length in mutants [$P < 0.005$ **(H)** and $P < 0.0001$ **(J)** by unpaired two-tailed *t*-test]. Scale bars: 250 μm **(E, E', I, I')**. LV, left ventricle.

(Fig. 3G, G', H) and by 33% in sagittal sections of lineage-traced mutants (Fig. 3I, I', J). These data indicate that haploinsufficiency of Dll4 in SHF leads to a reduction in the size of SHF-derived RV and length of SHF-derived OFT. This foreshortened OFT is unable to align itself over the developing RV and LV, such that the ensuing phenotype is an alignment defect, DORV.

Partial conditional loss of Dll4 expression leads to reduction in SHF progenitor cell pool

The observed reduction in the RV size and OFT length in mutants suggests that there is a reduction in the incorporation of SHF progenitor cells into the developing heart after heterozygous loss of *Dll4*. This could result from a reduction in the number of SHF progenitors available for incorporation or from an inability of available SHF cells to migrate into the developing heart. To directly address this question, we studied the size of the SHF progenitor pool. We lineage-traced SHF cells (*Islet1-Cre/R26R,tdT*) and studied the area occupied by tdT-positive cells in the SHF mesodermal region (Fig. 4A–C). Sagittal sections of mutant embryos showed a 56% reduction in tdT-positive cells in the SHF mesoderm. This would indicate that the observed reduction in the size of SHF-derived structures in the heart results from a loss of SHF progenitors available for incorporation into the developing heart. We then studied proliferation in lineage-traced SHF progenitors. To this end, control and mutant embryos in *Islet1-Cre/R26R,tdT* background were stained for pHH3. Double-positive cells in the region of the pharyngeal mesoderm were counted in controls and mutants. At E10.5 (Fig. 4D–F), heterozygous loss of *Dll4* resulted in a 33% reduction in proliferating SHF cells. Loss of proliferative potential in these early progenitor cells directs them toward apoptosis, and hence, we studied apoptosis in SHF cells with TUNEL staining. Partial loss of *Dll4* resulted in a fourfold increase in SHF progenitor cell apoptosis at E10.5 (Fig. 4G–I).

Discussion

Notch signaling is an evolutionarily conserved signaling pathway that plays important roles in cell fate specification, development, differentiation, and patterning in numerous cell types in the body. In mammals, there are four transmembrane Notch receptors (Notch 1–4) and five *trans*-membrane Notch ligands (Delta-like ligand 1, 3, 4 and Jagged 1 and 2) [19]. During canonical Notch signaling, a Notch receptor interacts in *trans* with its ligand expressed on a neighboring cell, leading to proteolytic cleavage of the receptor and subsequent nuclear translocation of the Notch intracellular domain (NICD) [20]. NICD forms a complex with CBF1/Suppressor of Hairless/LAG-1 (CSL) family of DNA binding proteins, which activates the transcription of cell-specific downstream effector molecules [20]. We and others have shown that Notch signaling plays a variety of different roles in cardiac development, in particular, OFT maturation. Early in heart development, Dll4 serves as the primary ligand of Notch 1 and plays a proliferative role in progenitor cells [11,21], similar to the pro-proliferative role of Dll4 in other progenitor beds, such as retinal [22] or neural progenitors [23]. Later in heart development, Dll4 expression wanes and Jagged1 takes over as the primary Notch ligand. Jagged-mediated Notch signaling regulates subsequent cardiac patterning [21]and maturation events such as epithelial-to-mesenchymal transformation in OFT cushions [24].

Notch pathway mutations have been implicated in several clinical CHDs. With particular reference to the OFT, Notch mutations have been identified in patients with bicuspid aortic valve [25,26] and aortic valve calcification [26]. Mutations in Jagged1 are causative in Alagille syndrome, which includes biliary malformations, and pulmonary artery defects [27]. Animal studies of Dll4 have shown that there is a dosage-sensitive requirement of Dll4 in arterial maturation, such that more than half the embryos with global Dll4 haploinsufficiency die in early gestation due to a vascular maturation arrest [15]. Likely due to this critical requirement of Dll4 during development, *Dll4* mutations have been infrequently reported in human diseases.

Recent evidence suggests a role for Dll4 in patients with AOS. Initial studies identified mutations in six genes in AOS: *Arhgap31*, *Dock6*, *Eogt*, *Rbpj*, *Notch1*, and *Dll4* [28]. Four of these genes (*Eogt, Rbpj, Notch1*, and *Dll4*) play a critical role in the canonical Notch pathway. Although autosomal recessive mutations in *Eogt* lead to AOS [28], the other three genes are believed to play an autosomal dominant role [8]. In a large study of targeted resequencing of *Dll4* gene with a custom enrichment panel in 89 independent families, nine heterozygous loss-of-function mutations in *Dll4* were identified [9]. This included two nonsense and seven missense mutations, all of which were thought to be critical for maintaining structural integrity of the protein. An

FIG. 4. Dll4 expression is required for SHF cell proliferation to maintain an adequate progenitor cell pool. The SHF cells were lineage traced by crossing R26R,tdT mice into Islet1-Cre line. Sagittal sections of control **(A, A')** and *Dll4* heterozygous mutant (*Islet1-Cre,Dll4*$^{F/wt}$) **(B, B')** embryos were evaluated at E10.5. The tdT-positive area (mean ± SEM) within the SHF mesodermal region (*boxed*) was normalized to control embryos **(C)**. Mutants demonstrated a 56% reduction in the SHF cell progenitor pool size compared with controls ($P < 0.05$). Transverse sections of Islet1 lineage-traced E10.5 control **(D)** and *Islet1-Cre,Dll4*$^{F/wt}$mutant **(E)** embryos were stained for pHH3 expression to study SHF proliferation in SHF cells. Higher magnification of *boxed area* in **D** and **E** is shown as lineage-traced Islet1 expression through tdT **(D', E')**, pHH3 expression **(D'', E'')** and merged image **(D''', E''')**. Islet1 and pHH3 double-positive cells were counted in 5 control and 5 mutant fields **(F**, mean, SEM**)**, showing a 33% reduction in proliferating SHF cells in mutants ($P < 0.005$). Similarly transverse sections of Islet1 lineage-traced E10.5 control **(G)** and *Islet1-Cre,Dll4*$^{F/wt}$mutant **(H)** embryos were stained by TUNEL to study SHF apoptosis. Higher magnification of *boxed area* in **G** and **H** is shown as lineage-traced Islet1 expression through tdT **(G', H')**, TUNEL staining **(G'', H'')**, and merged image **(G''', H''')**. Double-positive cells were counted in 4 control and 6 mutant fields within the *boxed region* **(I**, mean, SEM**)**, showing a fourfold increase in apoptosis in SHF in mutants ($P < 0.005$). Scale bars: 100 μm **(A', B', D'–E''', G'–H''')**, 250 μm **(A, B, D, E, G, H)**.

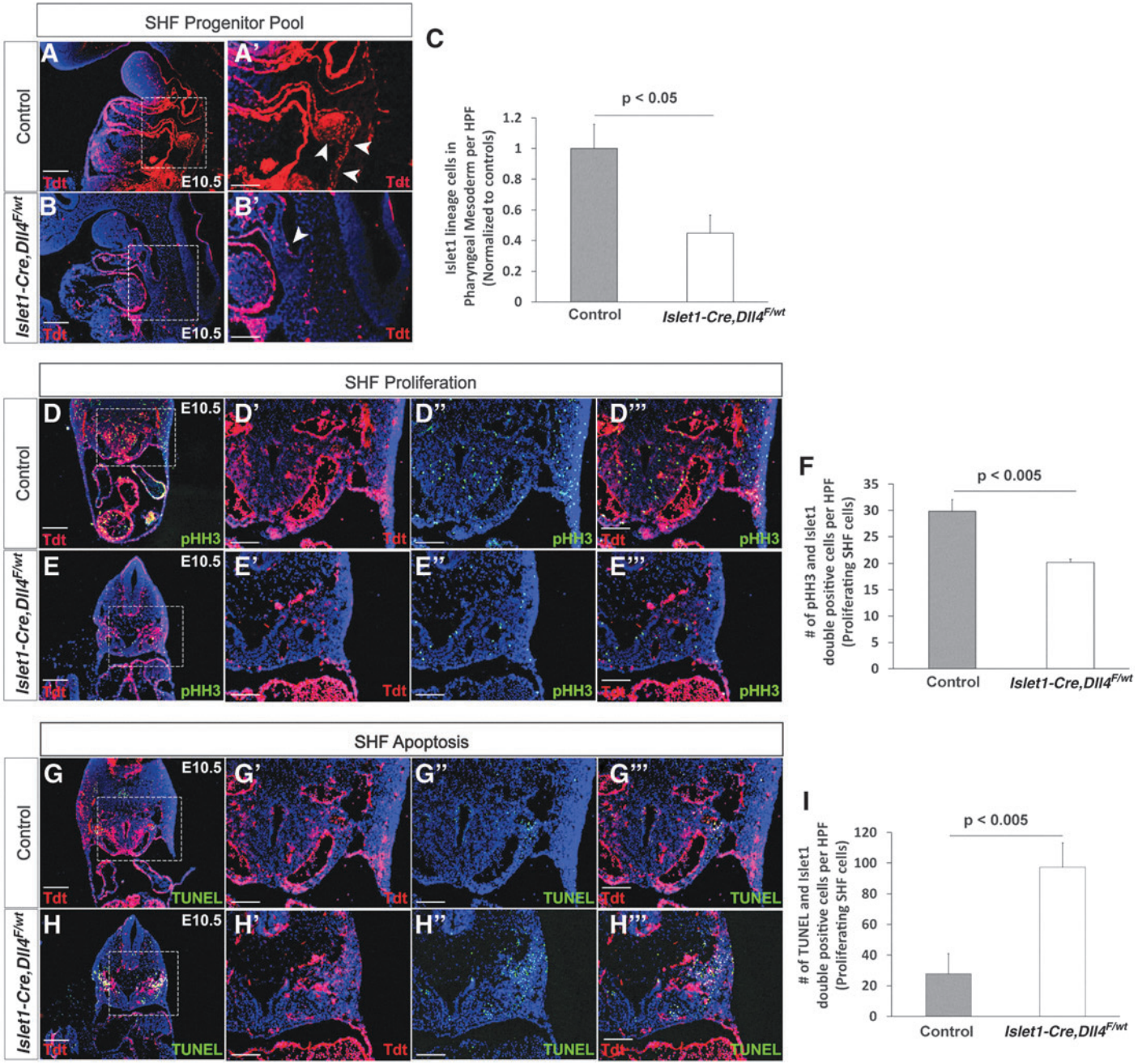
SHF Progenitor Pool
Control
Islet1-Cre,Dll4F/wt
A
A'
B
B'
Tdt
E10.5
C
p < 0.05
Islet1 lineage cells in Pharyngeal Mesoderm per HPF (Normalized to controls)
1.2
1
0.8
0.6
0.4
0.2
0
Control
Islet1-Cre,Dll4F/wt
SHF Proliferation
D
D'
D''
D'''
E
E'
E''
E'''
pHH3
F
p < 0.005
# of pHH3 and Islet1 double positive cells per HPF (Proliferating SHF cells)
35
30
25
20
15
10
5
0
Control
Islet1-Cre,Dll4F/wt
SHF Apoptosis
G
G'
G''
G'''
H
H'
H''
H'''
TUNEL
I
p < 0.005
# of TUNEL and Islet1 double positive cells per HPF (Proliferating SHF cells)
120
100
80
60
40
20
0
Control
Islet1-Cre,Dll4F/wt

additional missense mutation in *Dll4* that interferes with its binding to Notch1 has also been described in a sporadic Japanese patient [10]. However, no genotype–phenotype correlations have been made in AOS to date [9].

Almost one quarter of patients with AOS harbor a CHD, with the most common being outlet VSD or alignment defect, primarily TOF [7], both defects that can result from derangements in SHF contribution to the developing heart. Based on our current understanding of Dll4 biology, we submit that the cardiac defects seen in AOS are best explained by a somatic mutation acquired in mesodermal SHF progenitor cells after the initial steps in embryogenesis are effectively completed. We have previously shown that knockout of *Dll4* in SHF results in RV and OFT underdevelopment and early embryonic lethality [11]. The few embryos that survive to mid-gestation display DORV. We now wanted to model heterozygous *Dll4* loss in cardiac OFT-specific progenitor cells to establish a laboratory model of CHD seen in AOS. Islet1 is expressed early in heart development and globally by SHF progenitor cells destined to contribute to the developing heart. We, therefore, generated heterozygous conditional loss of *Dll4* in Islet1-expressing SHF cells. Haploinsufficiency of *Dll4* had demonstrable effects on SHF, with a significant reduction in SHF proliferation. The SHF progenitors incapable of proliferation subsequently undergo apoptosis, ultimately leading to a reduction in pool of SHF progenitors. We have previously shown that Dll4-mediated Notch signaling regulates Fgf8 and Fgf10 expression in SHF, thereby affecting SHF proliferation [11]. Loss of SHF progenitors available for incorporation into the developing heart leads to an underdeveloped RV and foreshortened OFT, leading to its misalignment. The aortic alignment defects seen in our model resemble the spectrum of defects seen in the clinic. In milder cases, the aorta rides across the VSD as seen in TOF, implying inadequate displacement to the LV. In more extreme cases, the aorta arises completely from the RV resembling TOF-style DORV. Thus, our model serves as the first molecular demonstration of the genotype–phenotype correlation of CHD observed in AOS.

The incomplete penetrance of CHD phenotype is consistent with *Dll4* biology. The penetrance of vascular defects in global Dll4 heterozygotes was shown to be strain-dependent [14], implying that there is likely epistatic regulation of Dll4 function, such that some individuals are able to overcome the impact of partial loss of Dll4. Our mouse model had a greater prevalence of CHD than reported in the clinic. One potential explanation is that the *Islet1-Cre* mouse used in our model is a cre recombinase knock-in, in effect acting as heterozygous loss of *Islet1*. This oligogenic mutation may underlie the increased penetrance observed. Alternatively, biological variability driven by the extent and degree of Dll4 loss could also be in play. Heterozygous loss of *Dll4* driven by *Mef2c-AHF-Cre*, a more restricted SHF marker, had no phenotype lending further credence to this argument. Lastly, our mouse model does not lend itself to studying associated defects in other organ systems. It has been suggested that the limb and scalp defects observed in AOS are a result of a more general vasculopathy [8]. It is well established that Dll4 plays a crucial role in vascular development and, further, that common mesodermal progenitors drive both vascular and cardiac development. Future studies aimed at establishing a laboratory model that displays the multi-organ system defects in AOS should shed more light into these aspects of the disease process.

Conclusion

In summary, we have established a laboratory model to explain the CHD observed in AOS due to heterozygous loss of function of *Dll4*. Our data indicate that a later and more regional loss of *Dll4* in SHF progenitors inhibits their proliferation, leading to reduced SHF incorporation in the developing OFT. A foreshortened OFT is incapable of proper alignment and, therefore, results in the cardiac alignment defects observed in the clinic. Our model would also imply that the RV in these mutants shares these molecular defects. As such, further studies would help us understand whether and how this abnormal RV would behave in the long term in patients who undergo surgical management of OFT CHD in AOS.

Author Disclosure Statement

No competing interests are declared.

Funding Information

This work was supported in part by NIH grants 5T32HD060549-05 to P.D.Z., F30HL154324 to O.T., and R03HL154301 and K08HL121191 to S.R.K.

Supplementary Material

Supplementary Table S1
Supplementary Table S2

References

1. Luxán G, G D'Amato, D MacGrogan and JL de la Pompa. (2016). Endocardial notch signaling in cardiac development and disease. Circ Res 118:e1–e18.
2. Vincent SD and ME Buckingham. (2010). How to make a heart. In: *Current Topics in Developmental Biology*. San Diego, CA: Elsevier, pp. 1–41.
3. Simeone RM, ME Oster, CH Cassell, BS Armour, DT Gray and MA Honein. (2014). Pediatric inpatient hospital resource use for congenital heart defects: costs congenital heart defects. Birth Defects Res Part A Clin Mol Teratol 100:934–943.
4. Neeb Z, JD Lajiness, E Bolanis and SJ Conway. (2013). Cardiac outflow tract anomalies. WIREs Dev Biol 2:499–530.
5. Zaidi S, M Choi, H Wakimoto, L Ma, J Jiang, JD Overton, A Romano-Adesman, RD Bjornson, RE Breitbart, et al. (2013). De novo mutations in histone-modifying genes in congenital heart disease. Nature 498:220–223.
6. Lehman A, W Wuyts and MS Patel. (2016). Adams-Oliver Syndrome. In: *GeneReviews® [Internet]*. Adam MP, Ardinger HH, Pagon RA, et al., eds. Seattle, WA: University of Washington, 1993–2021, https://www.ncbi.nlm.nih.gov/books/NBK355754/
7. Hassed S, S Li, J Mulvihill, C Aston and S Palmer. (2017). Adams-Oliver syndrome review of the literature: refining the diagnostic phenotype: Adams-Oliver syndrome: refining the phenotype. Am J Med Genet 173:790–800.
8. Stittrich A-B, A Lehman, DL Bodian, J Ashworth, Z Zong, H Li, P Lam, A Khromykh, RK Iyer, et al. (2014). Mutations in NOTCH1 cause Adams-Oliver syndrome. Am J Hum Genet 95:275–284.

9. Meester JAN, L Southgate, A-B Stittrich, H Venselaar, SJA Beekmans, N den Hollander, EK Bijlsma, A Helderman-van den Enden, JBGM Verheij, et al. (2015). Heterozygous loss-of-function mutations in DLL4 Cause Adams-Oliver syndrome. Am J Hum Genet 97:475–482.
10. Nagasaka M, M Taniguchi-Ikeda, H Inagaki, Y Ouchi, D Kurokawa, K Yamana, R Harada, K Nozu, Y Sakai, et al. (2017). Novel missense mutation in DLL4 in a Japanese sporadic case of Adams–Oliver syndrome. J Hum Genet 62:851–855.
11. De Zoysa P, J Liu, O Toubat, J Choi, A Moon, PS Gill, A Duarte, HM Sucov and SR Kumar. (2020). Delta-like ligand 4-mediated Notch signaling controls proliferation of second heart field progenitor cells by regulating Fgf8 expression. Development 147:dev185249.
12. Cai C-L, X Liang, Y Shi, P-H Chu, SL Pfaff, J Chen and S Evans. (2003). Isl1 identifies a cardiac progenitor population that proliferates prior to differentiation and contributes a majority of cells to the heart. Dev Cell 5:877–889.
13. Verzi MP, DJ McCulley, S De Val, E Dodou and BL Black. (2005). The right ventricle, outflow tract, and ventricular septum comprise a restricted expression domain within the secondary/anterior heart field. Dev Biol 287:134–145.
14. Benedito R and A Duarte. (2005). Expression of Dll4 during mouse embryogenesis suggests multiple developmental roles. Gene Expr Patterns 5:750–755.
15. Duarte A. (2004). Dosage-sensitive requirement for mouse Dll4 in artery development. Genes Dev 18:2474–2478.
16. Koch U, E Fiorini, R Benedito, V Besseyrias, K Schuster-Gossler, M Pierres, NR Manley, A Duarte, HR MacDonald and F Radtke. (2008). Delta-like 4 is the essential, nonredundant ligand for Notch1 during thymic T cell lineage commitment. J Exp Med 205:2515–2523.
17. Jiang X, DH Rowitch, P Soriano, AP McMahon and HM Sucov. (2000). Fate of the mammalian cardiac neural crest. Development 127:1607–1616.
18. Madisen L, TA Zwingman, SM Sunkin, SW Oh, HA Zariwala, H Gu, LL Ng, RD Palmiter, MJ Hawrylycz, et al. (2010). A robust and high-throughput Cre reporting and characterization system for the whole mouse brain. Nat Neurosci 13:133–140.
19. Andersson ER, R Sandberg and U Lendahl. (2011). Notch signaling: simplicity in design, versatility in function. Development 138:3593–3612.
20. de la Pompa JL and JA Epstein. (2012). Coordinating tissue interactions: notch signaling in cardiac development and disease. Dev Cell 22:244–254.
21. D'Amato G, G Luxán, G del Monte-Nieto, B Martínez-Poveda, C Torroja, W Walter, MS Bochter, R Benedito, S Cole, et al. (2016). Sequential Notch activation regulates ventricular chamber development. Nat Cell Biol 18:7–20.
22. Luo H, K Jin, Z Xie, F Qiu, S Li, M Zou, L Cai, K Hozumi, DT Shima and M Xiang. (2012). Forkhead box N4 (Foxn4) activates Dll4-Notch signaling to suppress photoreceptor cell fates of early retinal progenitors. Proc Natl Acad Sci U S A 109:E553–E562.
23. Rocha SF, SS Lopes, A Gossler and D Henrique. (2009). Dll1 and Dll4 function sequentially in the retina and pV2 domain of the spinal cord to regulate neurogenesis and create cell diversity. Dev Biol 328:54–65.
24. High FA, R Jain, JZ Stoller, NB Antonucci, MM Lu, KM Loomes, KH Kaestner, WS Pear and JA Epstein. (2009). Murine Jagged1/Notch signaling in the second heart field orchestrates Fgf8 expression and tissue-tissue interactions during outflow tract development. J Clin Invest 119:1986–1996.
25. McKellar SH, DJ Tester, M Yagubyan, R Majumdar, MJ Ackerman and TM Sundt. (2007). Novel NOTCH1 mutations in patients with bicuspid aortic valve disease and thoracic aortic aneurysms. J Thorac Cardiovasc Surg 134: 290–296.
26. Garg V. (2016). Notch Signaling in Aortic Valve Development and Disease. In: *Etiology and Morphogenesis of Congenital Heart Disease*. Nakanishi T, RR Markwald, HS Baldwin, BB Keller, D Srivastava, H Yamagishi, eds. Springer, Tokyo, Japan, pp. 371–376.
27. Li L, ID Krantz, Y Deng, A Genin, AB Banta, CC Collins, M Qi, BJ Trask, WL Kuo, et al. (1997). Alagille syndrome is caused by mutations in human Jagged1, which encodes a ligand for Notch1. Nat Genet 16:243–251.
28. Shaheen R, M Aglan, K Keppler-Noreuil, E Faqeih, S Ansari, K Horton, A Ashour, MS Zaki, F Al-Zahrani, et al. (2013). Mutations in EOGT confirm the genetic heterogeneity of autosomal-recessive Adams-Oliver syndrome. Am J Hum Genet 92:598–604.

Address correspondence to:
Dr. S. Ram Kumar
Department of Surgery
Keck School of Medicine
University of Southern California, Los Angeles
1520 San Pablo Street, Suite #4300
Los Angeles, CA 90033
USA

E-mail: rsubrama@usc.edu

Received for publication March 16, 2021
Accepted after revision April 22, 2021
Prepublished on Liebert Instant Online April 24, 2021